كلية الهندسة بشبرا
FACULTY OF ENGINEERING AT SHOUBRA
ERJ
PRINT ISSN 3009-6049
ONLINE ISSN 3009-6022

ENGINEERING RESEARCH JOURNAL (ERJ)
Volume (54),Issue (4)
October 2025, pp:59-77
https://erjsh.journals.ekb.eg

Hybrid Glass Powder-Silica Slurry for Enhanced Self-Compacting Concrete

Khaled A. M. Gharib [1,*], Amr A. Gamal [1], Mohamed I. Serag [2] , Mohamed O.R. Elhariri [1] , Mohamed A. S. Abd Elmageed [1]

[1] Faculty of Engineering at Shoubra, Benha University, Cairo, Egypt
[2] Faculty of engineering, Cairo University, Egypt
**Corresponding author*

E-mail address: khaled.Gharib@feng.bu.edu.eg, Amr.gamaleldin@feng.bu.edu.eg, dr.serag77@yahoo.com, Osama.alhariri@feng.bu.edu.eg, moha-ashraf@hotmail.com

Abstract: The construction industry requires improved concrete performance through sustainable solutions. The present study investigates the synergistic effect of Glass Powder (GP) and silica slurry (SS) hybridization in self-compacting concrete (SCC) to improve the mechanical and microstructural properties. Fourteen SCC test mixes with varying proportions of GP (5-20%) as sand replacement and SS (2.5-7.5%) as cement replacement were studied. Results showed 15% GP improved flowability by 26% and 90-day compressive strength by 78.6%. The optimum mix (15% GP + 5% SS, w/c ratio = 0.36) showed 55% reduced water absorption, indicating enhanced durability. Microstructural examination showed a denser matrix, with BET analysis confirming reductions in surface area and pore volume by 75.5% and 67.2%. Despite enhanced early-age performance, ettringite formation in the interfacial transition zone was observed to limit long-term strength development. Hybrid use of GP and SS has been shown to enhance both the mechanical behavior and sustainability of SCC.

Keywords: Self-compacting concrete; Glass powder; Silica slurry; Mechanical properties; and Microstructure.

1. Introduction

The construction industry continues to face growing challenges in balancing structural performance with environmental sustainability. As concrete is the second most consumed material globally after water, numerous studies have explored the use of supplementary cementitious materials (SCMs), particularly those derived from industrial waste, to reduce cement usage and enhance concrete performance. Among these, glass powder (GP) and silica slurry (SS) have emerged as promising materials due to their pozzolanic properties and their positive impact on both workability and durability. However, previous studies have yielded mixed and inconclusive findings regarding the individual and combined effects of GP and SS in self-compacting concrete (SCC), particularly when silica is introduced in slurry form rather than as a dry powder. This highlights the need for a systematic investigation into their synergistic behavior under controlled conditions.

Recent studies have investigated the application of waste-derived supplementary cementitious materials such as glass powder (GP) and silica-based admixtures to enhance concrete performance and sustainability. Glass powder, which is produced by grinding waste glass into particles smaller than 100 µm, comprises predominantly silica (SiO_2), sodium oxide (Na_2O), and calcium oxide (CaO). Its silica content is accountable for pozzolanic reactions with calcium hydroxide dissolved during cement hydration, forming additional calcium silicate hydrate (C–S–H) gel and increased mechanical strength and durability [1–11]. Silica fume (SF), a by-product of silicon and ferrosilicon alloy production, consists of ultrafine amorphous particles with a large specific surface area that enhance concrete strength, reduce permeability, and refine pore structure [12,13]. Although traditionally used as a dry powder, SF is also available in slurry form for easier handling, dispersion, and SCC compatibility [14,15]. Where workability is concerned, several studies have reported increased flowability in SCC when glass powder is introduced due to its low water absorption and dense surface texture [16–19]. The influence of silica-based additives on workability is more complex. Zinchenko et al. [20] reported improved flowability and segregation resistance with silica slurry, while Motahari et al. [21] observed decreased workability due to addition of slurry due to increased surface area of fine particles, and such effect could be minimized by adding high-range water-reducing admixtures. Yasser et al. [22] also observed increased slump flow with glass powder and decreased flow with silica fume. Keerio et al. [23] concluded that higher dosages of the two additives reduce workability, with silica having a more significant impact on it because of its smaller particle size. Mechanically, Abd El-Hameed et al. [24] concluded that replacement of 15% of cement with glass powder increased compressive strength by up to 28.6% at 28 days. Khatib et al. [25] concluded that there were improvements with 10% replacement but major losses from 20% or more. Nassar and Soroushian [26] demonstrated that ground glass addition improved the strength of recycled aggregate concretes through better microstructure and interfacial transition zone. Ramezanianpour et al. [27] reported that 8% silica slurry provided higher compressive and splitting tensile strengths compared to blended cement mixes, contributed primarily by enhanced particle dispersion and a denser ITZ. However, they noted that silica fume's pozzolanic activity is greatest at young ages with very small differences in strength gain after 28 days. Tests have also shown that glass powder and silica additives account for reduced water absorption and denser microstructures [23,30]. Microstructural studies [24,29] concluded that pozzolanic reactions between SCMs and calcium hydroxide generate more C–S–H gel, hence denser matrices and enhanced durability.

While extensive research has documented the individual effects of glass powder and silica-based materials, a critical knowledge gap remains regarding their simultaneous use in self-compacting concrete. The synergistic mechanisms of glass powder-silica slurry hybridization under controlled low w/c ratios are fundamentally unexplored. This study directly addresses this gap by investigating their combined effects on mechanical and microstructural properties.

This study presents a novel approach to developing sustainable high-performance self-compacting concrete (SCC) by focusing on two primary aspects. First, it investigates the optimization of the water-to-cement ratio to achieve maximum particle packing density and minimize porosity. Second, it systematically evaluates the synergistic effects of ground granulated blast-furnace slag (GP) and silica slurry (SS) on the fresh, mechanical, and microstructural properties of SCC mixtures. The utilization of silica slurry is anticipated to enhance dispersibility and mitigate the agglomeration issues commonly encountered with dry supplementary cementitious materials (SCMs). By thoroughly analyzing the performance of GP-SS hybrid systems, this research aims to significantly contribute to the understanding of sustainable strategies for manufacturing advanced SCC.

The main objectives of this study are to:

- Identify the optimal replacement levels of GP and SS to enhance the workability and strength of SCC.
- Examine the influence of varying water-to-cement ratios on the packing density and porosity of the concrete matrix.
- Compare the performance of hybrid GP-SS mixtures with control and single-admixture concrete formulations under controlled laboratory conditions.

2. Experimental Program

2.1 Material Description

2.1.1 Ordinary Portland Cement (CEM I 42.5N)

This traditional Portland cement meets ASTM C150 Type I specifications with a compressive strength of 42.5 MPa and specific gravity of 3.15.

2.1.2 Fine Aggregate

Natural sand from the Nile River basin by the ASTM C33 specification. Specific gravity 2.6, particle size maximum 4.75mm, absorption 1.2%. Particle size distribution as per ASTM C136. Gradation curve within the limits of ASTM C33, indicating well-graded aggregate.

2.1.3 Coarse Aggregate

Dolomite crushed, Egypt, Gebel Ataqa Quarries, ASTM C33. Specific gravity 2.5, max. particle size 12.5mm, water absorption 0.5%. The particle size distribution curve is as in Figure 1. Aggregate enhances the strength and durability of concrete.

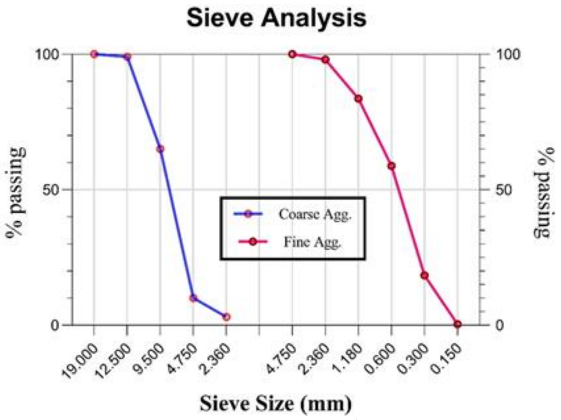

Figure 1: Particle size distribution curves of coarse aggregate and sand.

2.1.4 Glass Powder (GP)

White, clear, high-purity glass powder as a sand substitute. Ground and pulverized glass to a 5.5-micrometer particle size, as measured by the Dynamic Light Scattering. Glass powder was substituted with some fine aggregate to improve the characteristics. Fineness enhances pozzolanic activity and packing of the concrete. Table 1 is a comprehensive Glass Powder attributes for consideration of suitability as an additive cement.

2.1.5 Silica Slurry

The concrete mix designs in this study incorporated Sika® Fume Slurry, a high-fineness silica fume suspension in water, as a partial cementitious replacement in the SCC mixtures. The slurry consists of ultra-fine, reactive silica particles with an average diameter of approximately 0.1 µm. It contains 50% solid content and has a specific gravity of 1.38. Visually, it appears as a uniform grey suspension.

The extremely small particle size provides a large surface area, which enhances pozzolanic reactions and contributes to improved concrete strength and long-term durability. The slurry formulation also allows for better dispersion and homogeneity within the cementitious matrix, leading to a denser and more refined microstructure. Chemical analysis has shown that the slurry contains less than 0.10% chloride ions, classifying it as virtually chloride-free. Furthermore, its sodium oxide equivalent is 0.16%, indicating a low alkali contribution. The silica slurry content is shown in Table 1.

Table 1: Chemical Composition of Glass Powder, cement, and Silica slurry Analyzed by (XRF Test Results)

Compound	Glass %	Cement %	Silica Slurry %
SiO_2	72.22	20.8	49.8
Na_2O	13.6	0.22	0.1
CaO	11.5	63.9	0.03
MgO	0.32	2.3	0.02
Al_2O_3	1.9	5.2	0.03
K_2O	0.35	0.82	0.01
Fe_2O_3	0.07	3.1	0.02
TiO_2	0.04	0.26	0.01
SO_3	-	2.4	0.01
H_2O	-	-	49.95

2.1.6 Chemical Admixtures

Sika Visco Flow® 102: Performance admixture that increases plasticity and slump retention. Next-generation polycarboxylate polymer technology delivers increased plasticity and longer slump retention with no additional cost. Use for precast/prestressed and ready-mix conventional, high-slump, and Self-Compacting Concrete applications. Maintains slump life with no cement hydration retardation. Specific gravity 1.05 g/cm³, reddish liquid form. A constant dosage of 11.3 kg/m³ was applied to all mixtures based on preliminary optimization trials. This fixed dosage strategy enabled systematic evaluation of GP and SS rheological effects while ensuring adequate workability (target slump flow: 650-750 mm) across all combinations.

2.2 Mixes Features

Study variables applied in a mixed design and testing of SCC mixtures shown in Table 2. Slump flow, L-box, J-ring, and GTM tests were part of fresh property tests. Raw materials (Portland cement, aggregates, glass powder, dry components) batched, then variable mold sizes set up: cubes 100×100×100mm, cylinders ϕ100×200mm height, beams 70×140×500mm for the demonstration of the precision of the tests.

2.3 Casting and curing of specimens

SCC mixes are prepared according to the standardized mix procedure. Materials and water mixed with admixtures, mixed for 6 minutes. Pre-casting property testing. Two-stage curing: 24-hour initial, followed by standard curing at 7, 28, 56, and 90 days as per ASTM C31**.** Three cubic specimens (100×100×100 mm) were prepared for each mixture at each test age (7, 28, 56, and 90 days) for compressive strength testing. Three cylindrical specimens (ϕ100×200 mm height) were prepared for splitting tensile strength testing, and three prismatic beam specimens (70×140×500 mm) were prepared for flexural strength testing, both tested at 28 days. Durability tests (water absorption and sorptivity) were conducted at 90 days on the optimal mixture from each group based on mechanical strength results, using two cubic specimens per mixture. Microstructural analysis samples (SEM, XRD, BET) were obtained from cubic specimens of the optimal mixtures after compressive strength testing.

2.4 Testing Methods

2.4.1 Fresh properties

Four standard tests defined SCC fresh properties: Slump flow test (EN 12350-8) for filling capacity and flowability; J-Ring test (EN 12350-12) for passing through confined space ability; L-Box Test (EN 12350-10) for flow behavior of reinforcing bar; GTM Test (EN 12350-11) for dynamic segregation resistance. Tests provide workability, cohesiveness, and stability values for advanced mixture proportions.

2.4.2 hardened properties

Mechanical tests as per ASTM standards: Tests for compressive strength Figure 2-a), (ASTM C39) to withstand axial loads; Tests for tensile strength on split cylinder Figure 2-b), (ASTM C496) to withstand tension; Tests for flexural strength Figure 2-c), (ASTM C78) to withstand bending. Completely detail the mechanical properties for structural applications.

2.4.3 Durability Characteristics

Water absorption properties tested by ASTM. Sorptivity test (ASTM C1585) evaluates the capillary water absorption rate and pore structure properties. Lower sorptivity values indicate better durability. Water absorption test (ASTM C-642) indicates porosity. Lower absorption rates indicate better long-term durability**.**

2.4.4 Microstructural

SEM scanning with JEOL JSM-7600F instrument combined with energy-dispersive X-ray spectroscopy for elemental analysis. Stereo microscopy with Nikon SMZ1500 stereomicroscope for surface topography. X-ray diffraction with Bruker D8 Discover for crystalline phase identification. XRF analysis with Oxford Instruments X 7200 spectrometer. Light scattering data with Zetasizer for particle size distribution. BET surface area determination with Nova Touch 2X gas sorption analyzer. Methods provide structural information and component relationships.

Table 2: Mix design proportions for Self-Compacting Concrete (SCC) mixtures.

NO of Mix	Label	Cement kg/m^3	Fine Agg kg/m^3	CoarseAgg kg/m^3	w.c kg/m^3	Glass Powder kg/m^3	Slurry kg/m^3	Vma kg/m^3
--	SCC- Control	450	859.12	966.5	175.5	0	-	11.3
Group1 Glass Powder								
1	SCC- G.P 5%	450	816.12	966.5	175.5	43	-	11.3
2	SCC- G.P10%	450	773.21	966.5	175.5	85.9	-	11.3
3	SCC- G.P15%	450	730.25	966.5	175.5	128.9	-	11.3
4	SCC- G.P20%	450	687.3	966.5	175.5	171.8	-	11.3
Group2 Silica Slurry								
5	SCC-SS-2.5%	438.8	859.12	966.5	171.13	-	11.3	11.3
6	SCC-SS-5%	427.5	859.12	966.5	166.72	-	22.5	11.3
7	SCC-SS-7.5%	416.3	859.12	966.5	162.35	-	33.8	11.3
Group3 Glass Powder Silica Slurry								
8	SCC-5%GP+5%SS	427.5	816.12	966.5	166.72	43	22.5	11.3
9	SCC-10%GP+5%SS	427.5	773.21	966.5	166.72	85.9	22.5	11.3
10	SCC-15%GP+5%SS	427.5	730.25	966.5	166.72	128.9	22.5	11.3
Group4 Glass Powder Silica Slurry (w.c%0.36)								
11	SCCL-5%GP+5%SS	427.5	816.12	966.5	153.9	43	22.5	11.3
12	SCCL-10%GP+5%SS	427.5	773.21	966.5	153.9	85.9	22.5	11.3
13`	SCCL-15%GP+5%SS	427.5	730.25	966.5	153.9	128.9	22.5	11.3

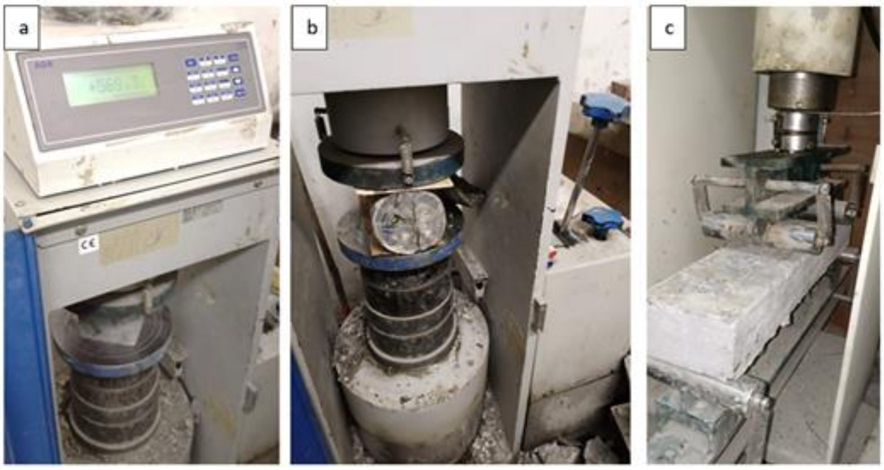

Figure 2: Testing equipment for **(a)** compressive, **(b)** tensile, and **(c)** flexural strength of Self-Compacting Concrete.

3. Results and Discussion

3.1 Fresh Concrete Properties

3.1.1 Slump Flow Test and T500

The slump flow and T500 results exhibit characteristic rheological mechanisms related to the addition of glass powder (GP) and silica slurry (SS) in self-compacting concrete (SCC). Table 3 and Figure 3 present comprehensive data on fresh properties of all SCC mixtures. In Group 1, the addition of GP systematically enhanced flowability due to a ball-bearing effect caused by the spherical particle morphology. At 20% GP replacement, the slump flow was raised from 555 mm for the control mix to 700 mm (improvement of 26%). This is far greater than the 15–18% range found by Aliabdo et al. [31] with conventional concrete. Moreover, the decrease of T500 from 6 to 4 seconds confirms improved viscosity and reduced inter-particle friction.

In Group 2 mixtures with SS, the slump flow reached 650 mm at 7.5% replacement and T500 decreased to 2 seconds. This improvement is attributed to enhanced particle dispersion and increased packing density. Arshad M.T. et al.

[32] reported that the incorporation of silica fume reduced SCC flowability and increased the demand for superplasticizers due to its high surface area and water absorption capacity. In contrast, well-dispersed silica slurry improved the fresh-state rheological behavior of SCC.

The synergistic effect of SS and GP in Group 3 was very remarkable. The maximum slump flow reached 710 mm, and the optimal viscosity was 2 seconds with 5% SS + 15% GP. This improvement is attributed to the ability of SS to reduce agglomeration of GP particles and enhance their dispersion within the cementitious matrix, inducing further lubrication and flowability enhancement. These results are different from those of Said et al. [33], in which nano-silica alone yielded only modest workability improvements.

In Group 4, the performance at lowered water content (w/c = 0.36) showed good water efficiency. Despite 10% less mixing water, the hybrid GP–SS system attained a slump flow of 610 mm, showing that dual lubrication and improved packing efficiency maintain workability even at low water contents. Significantly, this has not been achieved by earlier research efforts, like those of Du and Tan [34], on individual glass powder applications.

Overall, the hybrid rheological system integrates the physical ball-bearing effect of GP with the chemical viscosity modification provided by SS. The dual mechanism facilitates improved water efficiency and workability performance over traditional single-admixture strategies, substantiating its feasibility for high-performance SCC applications.

Table 3: Fresh properties of SCC mixtures with varying glass powder and liquid silica slurry content

No Of Mix	slump flow D mm	T500 sec	L-box h2/h1 mm	J-ring test Δ(H)mm	GTM-test %
Scc-con.	555	6	0.8	5	6%
Group1 Glass powder					
Scc-5% GP	577	5	0.82	5	6.70%
Scc-10% GP	620	5	0.85	0	7.50%
Scc- 15% GP	645	4	0.93	10	13.90%
Scc-20% GP	700	4	1	10	15.20%
Group2 Silica Slurry					
Scc-S-2.5%	600	5	0.81	3	8%
Scc-S-5%	630	3	0.825	5	9.30%
Scc-S-7.5%	650	2	0.84	7.5	15.20%
Group3 Silica Slurry+ Glass Powder					
Scc-S5%+5%GP	660	4	0.8587	8	18.50%
SCC-S5%+10%GP	690	2	0.95	10	20%
SCC-S5%+15%GP	710	2	1	10	21%
Group4 Silica Slurry+ Glass Powder (W.C% 0.36)					
SCC-L-S5%+5%GP	560	6	0.85	6	7%
SCC-L-S5%+10%GP	580	5	0.95	8	9%
SCC-L-S5%+15%GP	610	5	1	10	12%

According to EN 12350, the acceptance criteria for SCC fresh properties are: slump flow (SF1: 550-650 mm, SF2: 660-750 mm, SF3: 760-850 mm), L-box passing ratio (h2/h1) ≥ 0.8, J-Ring blocking step (PJ1: ≤ 10 mm, PJ2: ≤ 20 mm) with maximum difference from slump flow ≤ 50 mm, and GTM segregation resistance (SR1: ≤ 20%, SR2: ≤ 15%).

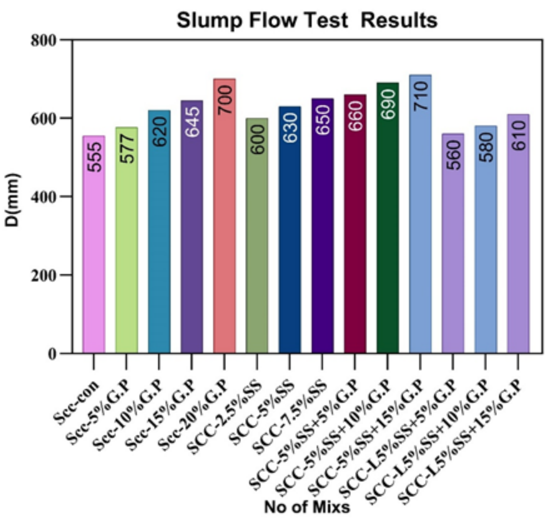

Figure 3: Slump flow test results for different mix designs.

3.1.2 J-Ring and L-Box Test

Table 3 presents fresh properties of SCC mixtures with varying glass powder and silica slurry content. **Group 1 (GP alone)** exhibited L-box ratios increasing from 0.82 at 5% GP to 1.00 at 20% GP, but J-Ring height difference increased from 5 mm to 10 mm, indicating that additional glass powder enhances flowability but makes passing ability through narrow sections more challenging due to particle adhesion and reduced lubrication, contrary to Aliabdo et al. [31] observations in conventional concrete. **Group 2 (SS alone)** displayed L-box ratios slightly increasing from 0.81 (2.5% SS) to 0.84 (7.5% SS), while height differences increased from 3 mm to 7.5 mm, as silica slurry enhances cohesion and prevents segregation. In contrast, Arshad M.T. et al. [32] reported that increasing silica fume content in SCC reduced flowability.

Group 3 (GP+SS) exhibited the best overall performance with optimum at 5% SS + 15% GP combination: L-box ratio of 1.00, height difference of 10 mm, and slump flow of 710 mm. Glass powder acts as a lubricant and reduces the viscosity increase caused by silica slurry, and the slurry facilitates even dispersion of glass particles by promoting particle interaction. This synergy creates better performance than individual additives used independently, as shown by Said et al. [33].

Group 4 with reduced w/c ratio (0.36) retained efficient performance, with L-box ratios ranging from 0.85 to 1.00 and height differences of 6-10 mm for varying GP levels (5-15%), indicating that GP-SS combination preserves passing ability despite 10% reduction in mixing water through enhanced particle interaction in concentrated paste systems, an effect not previously observed by Du and Tan [34].

3.1.3 GTM (Segregation Test)

Table 3 and Figure 4 present comprehensive fresh property data. According to EN 12350-11, acceptable segregation resistance requires GTM ≤ 15% (SR2 limit).

Group 1 (GP only) showed acceptable segregation resistance up to 10% GP (7.5% GTM) but deteriorated at higher dosages. At 15% GP, segregation reached 13.9%, approaching the safety limit, while 20% GP exceeded it at 15.2% despite achieving highest slump flow (700 mm). Glass particles enhanced flowability through ball-bearing mechanisms but progressively compromised paste cohesion by creating preferential flow channels and reducing inter-particle friction at higher levels, contrasting with Aliabdo et al. [31] findings in conventional concrete. **Group 2 (SS only)** demonstrated superior segregation resistance at lower dosages, with 5% SS achieving optimal performance: 630 mm slump flow (13.5% increase) and only 9.30% segregation significantly lower than 13.9% for 15% GP. However, 7.5% SS increased segregation sharply to 15.2%, matching the 20% GP threshold. This stems from finer silica particles initially forming denser paste matrices and enhancing cohesion through C-S-H formation while serving as nucleation sites, though excessive SS increases viscosity beyond optimal levels, causing particle agglomeration. These moderate-dosage benefits exceed silica fume improvements documented by Gao et al. [32].

Group 3 (GP+SS) revealed substantial limitations, where minimal hybrid content (5%SS+5%GP) produced 18.5% segregation, well exceeding the safety threshold despite 660 mm slump flow. Performance deteriorated with increasing GP content, reaching 20.0% at 10%GP and 21.0% at 15%GP. While workability increased dramatically (up to 710 mm), stability deteriorated as GP's lubricating effects counteracted SS's binding properties. Despite enhanced flowability, the hybrid system at standard w/c demonstrates antagonistic rather than synergistic behavior, producing worse stability than either additive individually, an issue not observed in Said et al. [33] research.

Group 4 (w/c=0.36) provided an effective solution, enabling acceptable segregation control across all dosages. Even at the highest level (15%GP+5%SS), segregation remained at 12%, safely below the threshold, while maintaining adequate workability (610 mm). Reduced water content effectively mitigates instability by producing denser paste and stronger particle interactions through enhanced packing and reduced bleeding, a strategy not explored by Du and Tan [34]. Group 4's balanced performance represents true synergistic behavior, achieving both adequate flowability (610 mm) and acceptable stability (12% GTM), demonstrating that proper mix optimization is essential for realizing hybrid SCM benefits.

Figure 4: Segregation Test Results for various concrete mix designs.

3.2 Hardened Concrete Properties

3.2.1 Compressive Strength

Table 4 and Figure 5 show the results of the mechanical properties of self-compacting concrete (SCC) mixes. (GP) and silica slurry (SS), producing complex strength development patterns across the four evaluated groups. These results were further confirmed by microstructural observations using SEM analysis (Figure 9). Group 1 (Figure 5a) (15% GP replacement of fine aggregate) exhibited efficient performance, achieving compressive strength gains of 24% in 7 days and 78.6% at 90 days. This outcome surpassed the 15–20% improvements reported by Khan et al. [35] and the 22.5% gains reported by Yahia et al. [36]. The superior performance is attributed to the dual mechanism of GP, combining a physical filler effect with pozzolanic reactivity that generates additional C–S–H gel. SEM analysis confirmed the presence of a dense microstructure, where glass particles acted as nucleation sites, accelerating cement hydration. Enhanced pore refinement and improved particle packing contributed to long-term strength development and durability. Group 2 (Figure 5b) (7.5% liquid SS as cement replacement) demonstrated moderate compressive strength gains of 11.1% at 7 days and 23.8% at 90 days. These results showed better long-term development than the early gains (18–20%) observed by Badalyan et al. [37], although the strength plateaued over time due to depletion of available $Ca(OH)_2$. The early improvements were primarily caused by rapid interfacial transition zone (ITZ) densification and ettringite formation. Notably, the use of liquid SS provided better workability and reduced segregation compared to conventional silica fume powder. Group 3 (Figure 5c) (Hybrid SCC containing 5% SS + 15% GP) achieved high early-age strength, with increases increase of 40.7% at 7 days, 27.6% at 28 days, and 47.6% at 90 days. These values exceeded the 25–30% reported by Raveendran et al. [38] and the 35–42% gains observed by Abraham et al. [6]. The observed synergy between GP and SS enhanced early hydration kinetics, despite SEM imaging revealing localized porosity that suggested some interference between the two mechanisms. Overall, the combination produced significant early strength while maintaining satisfactory flowability. Group 4 (Figure 5d) (Optimized hybrid SCC with a low w/c ratio of 0.36) demonstrated remarkable early compressive strength, reaching a 55.5% increase at 7 days. This performance exceeded 48.35 19 MPa reported by Paruthi et al. [39]. SEM analysis revealed a fine, dense microstructure with well-developed ettringite crystals. However, the extreme matrix density appeared to restrict long-term C–S–H development. Nevertheless, the optimized water-to-cement ratio significantly improved early-age strength while preserving self-compacting properties. Based on these results, it is recommended to use the SCC formulation containing 5% SS and 15% GP at low w/c ratios for applications requiring early formwork removal. Conversely, SCC mixtures incorporating 15% GP alone may be preferred where maximum long-term strength and durability are priorities, as confirmed by microstructural analysis.

3.2.2 Splitting Tensile and Flexural Strength

The flexural and splitting tensile strength results of the four SCC groups with GP and SS incorporation (Figure 6) showed variations in performance attributed to different microstructural mechanisms. Group 1(Figure 6-a) (SCC–15% GP) showed 65% flexural and 38.4% splitting tensile strength enhancements due to improved particle packing, reduced porosity, and effective crack-bridging by finer glass particles enhancing stress transfer across the matrix, with SEM observations confirming homogeneous microstructure with reduced weak zones and improved interfacial bonding, in agreement with Khan et al. [35], Yahia et al. [36], and Semmana et al. [40]. Group 2(Figure 6-b) (SCC–7.5% SS) showed 45% flexural and 46.2% tensile strength improvements due to pozzolanic activity and ITZ densification, with slurry form SS improving particle dispersion and reducing bleeding compared to powder counterpart, the results being comparable with conventional silica fume by Badalyan et al. [37] and improved C–S–H formation contributing significantly to tensile capacity and crack resistance. Group 3 (Figure 6-c) (SCC–15% GP + 5% SS) showed synergistic response with 50% flexural and 31.1% tensile strength improvements, though GP-SS combined action introduced complex microstructural interactions compromising long-term tensile efficiency to some extent with similar limitations in hybrid systems reported by Raveendran et al. [38] and Abraham et al. [41], where early-age strength was improved but matrix heterogeneity influenced tensile performance with time. Group 4 (Figure 6-d) (SCC–L–15% GP + 5% SS with lowered w/c) showed better overall performance as the best mix with 57.5% flexural and 36.2% tensile strength improvements, where lowered water content resulted in a denser matrix, better binder-aggregate bond, and lower permeability, exceeding flexural (5.01 MPa) and tensile (4.91 MPa) strengths normally obtained in high-grade geopolymer concretes reported by Paruthi et al. [39]. This optimized low w/c hybrid mix is the best combination for the attainment of maximum flexural and tensile strength performance.

Table 4: Mechanical Properties of Self-Compacting Concrete (SCC) Mixes with Various Additives.

No of mix	Compressive strength N/mm^2 7days	Compressive strength N/mm^2 at 28 days	Compressive strength N/mm^2 at 56-days	Compressive strength N/mm^2 at 90 days	splitting strength N/mm^2 at 28 days	Flexural strength N/mm^2 at 28-day
Scc-con.	27	38.2	41	42	3.18	4
Group 1 Glass Powder						
Scc-5% GP	30	46.5	54	56	3.5	4.4
Scc-10% GP	31	50	59	67	3.9	5.8
Scc-15% GP	33.5	55	67	75	4.4	6.6
Scc-20% GP	31.4	50.8	60	68	3.9	6.02
Group 2 Silica slurry						
Scc-2.5% SS	27	39	45	45	3.4	4.15
Scc-5% SS	28.5	44	49	49	4	5
Scc-7.5% SS	30	49	52	52	4.65	5.8
Group 3 Glass Silica Slurry						
Scc-5% GP+5% SS	31.5	42	50	50	3.6	5.22
Scc-10% GP+5% SS	35.5	45.87	56	56	3.92	5.7
Scc-15% GP+5%SS	38	48.74	62	62	4.17	6
Group 4 Glass+ Silica Slurry (w.c % 0.36)						
Scc-L-5% GP+5% SS	35	44.87	53	53	3.81	5.5
Scc-L-10% GP+5% SS	37	48	60	60	4	6
Scc-L-15% GP+5% SS	42	51	65	65	4.33	6.3

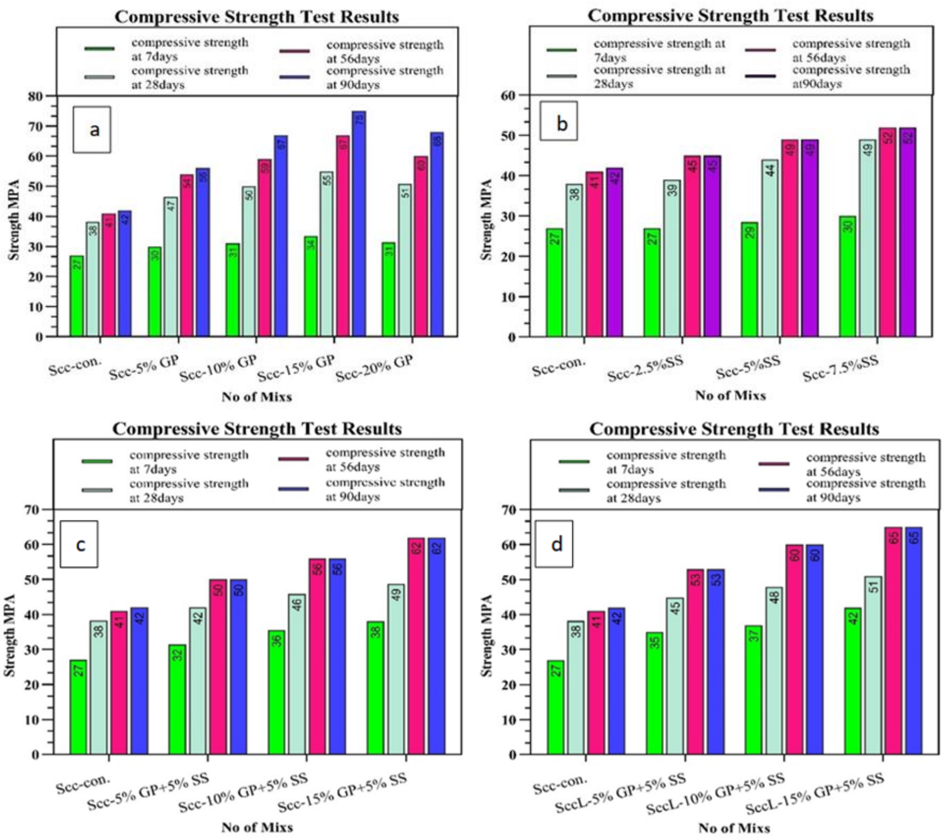

Figure 5: Comparative analysis of compressive strength development for various concrete mix designs across four distinct groups: **(a)** Group 1, **(b)** Group 2, **(c)** Group 3, and **(d)** Group4

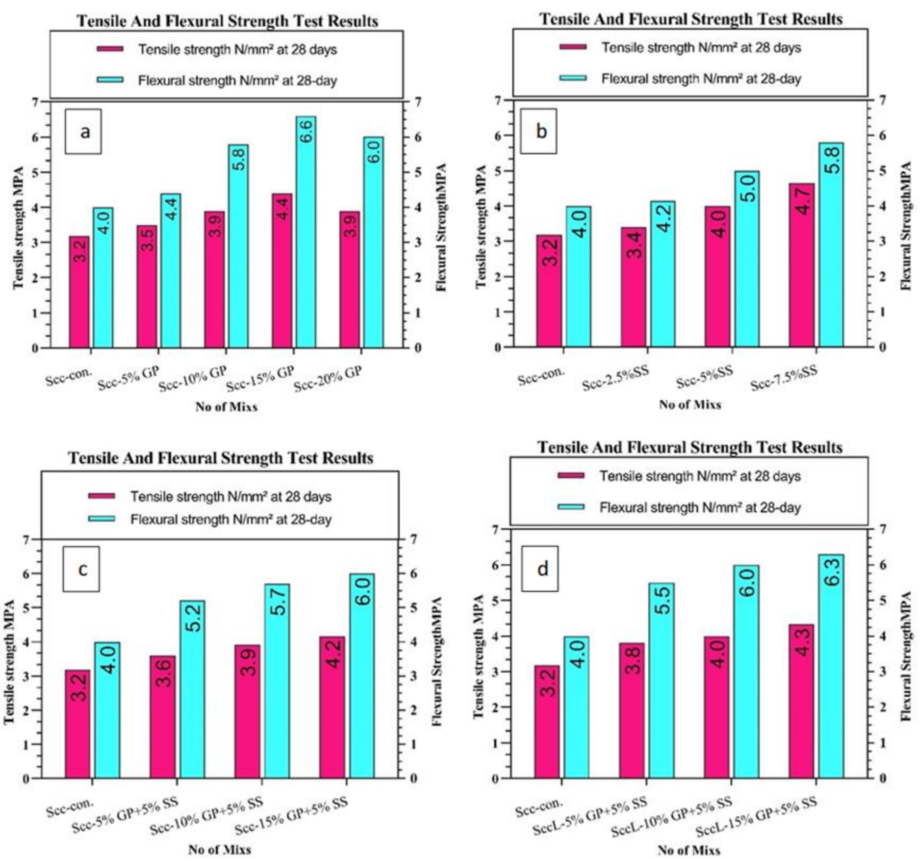

Figure 6: Comparison of flexural and splitting tensile strength development across different mix designs.: (a) Group1, (b) Group2, (c) Group3, and (d) Group4

3.3 Durability Characteristics

3.3.1 Water Absorption

Water absorption results (Figure 7) demonstrate that GP and SS significantly enhance the impermeability of SCC. The control mixture exhibited the highest absorption (40 grams), with porous microstructure and cracks providing direct water ingress paths.

Group 1 (15% GP) reduced absorption by 22% to 31 grams through filler effect and nucleation capability of dispersed glass particles, resulting in additional C-S-H gel formation and improved pore refinement, consistent with Kumar et al. [42] findings using glass powder in eco-friendly SCC. Group 2 (7.5% SS) achieved a 37.5% reduction (25 grams). The highly reactive, uniformly dispersed silica particles developed dense C-S-H structures that decreased pore connectivity and enhanced impermeability, comparable to Wang et al. [43] results with nano-silica in SCC.

Group 3 (15% GP + 5% SS) exhibited the most significant improvement with a 50% reduction (20 grams) despite a higher measured pore volume (1.186 cm³/g). While overall porosity increased, the pore structure became less connected and more tortuous, limiting water transport and highlighting the complex porosity-permeability relationship. Group 4 (15% GP + 5% SS, w/c=0.36) showed optimal performance with 55% reduction (18 grams), achieving an extremely dense, uniform matrix with improved particle distribution. Optimized w/c ratio and synergistic SS-GP interaction minimized total pore volume to 0.393 cm³/g, like impermeable microstructures reported by Kashyap et al. [44] with nano-silica and glass powder combinations.

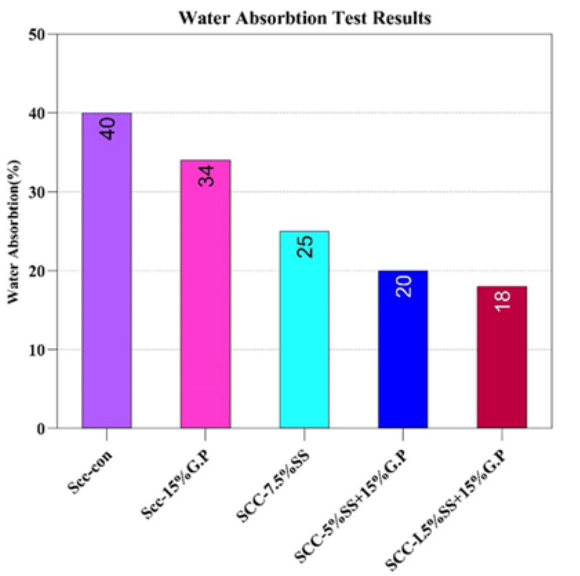

Figure 7: Comparison of water absorption results for SCC mixtures.

3.3.2 Sorptivity

Sorptivity results (Figure 8) demonstrate improved capillary water absorption resistance through GP and SS incorporation. The sorptivity coefficient ($I = Q/A\sqrt{t}$, where Q is cumulative absorption, A is exposed area, and t is time) indicates resistance to water penetration, with lower values representing better performance. The control mixture exhibited the highest sorptivity (I = 0.14 mm). Group 1 (15% GP) achieved a 35% reduction (I = 0.09 mm) due to GP's physicochemical characteristics and fine particle distribution, improving microstructural packing, supporting Aruchamy et al. [42] findings. Group 2 (7.5% SS) showed maximum reduction among single additives at 50% (I = 0.07 mm), where high specific surface area enabled pozzolanic reactions producing C-S-H gel that densified the matrix and decreased capillary porosity, consistent with Labaran et al. [45] and Wang et al. [43]. Group 3 (15% GP + 5% SS) demonstrated a 42.8% reduction (I = 0.08 mm), indicating synergistic benefits, though slightly lower than SS alone, suggesting material interference and suboptimal particle packing. Group 4 (15% GP + 5% SS, w/c=0.36) recorded the most notable improvement with 71% reduction (I = 0.04 mm), where reduced water content optimized particle packing and enhanced GP-SS synergy, confirming Kashyap et al. [44] conclusions. Groups 2 and 4 exhibited superior microstructural characteristics, including dense homogeneous matrix, optimal particle distribution, enhanced C-S-H formation, and reduced cracking, demonstrating that optimized silica slurry content and reduced w/c ratios significantly improve microstructure, mechanical response, and durability.

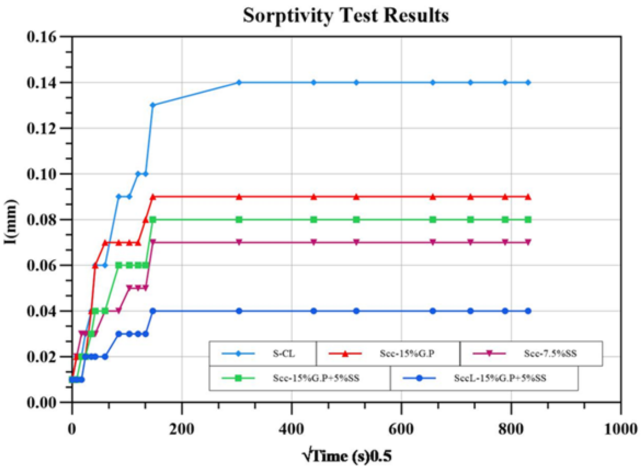

Figure 8: Sorptivity curves for different mixes over time

3.4 Microstructural Analysis

3.4.1 Scanning Electron Microscopy (SEM)

SEM analysis presented clear microstructural improvement in all SCC mixes, with clear relationships between pore structure enhancement and mechanical behavior. The control mixture (SCC-CON, Figure 9a) exhibited internal defects, including extensive crack networks, heterogeneous matrix, and poorly bonded interfaces characterized by large voids, resulting in high BET surface area measurements of 396.2 m²/g and total pore volume of 1.1977 cc/g, explaining the reduced mechanical performance. Group 1 (SCC–15% GP, Figure 9b) showed a notable microstructural weaknesses with homogeneous distribution of glass particles and dense C–S–H gel formation, achieving 90.4% reduction in BET surface area (38.2 m²/g) and 88.1% reduction in pore volume (0.143 cc/g), where glass particles acted as effective nucleation sites with firm adhesion to cement matrix and absence of microcracks confirmed enhanced structural integrity supporting the 78.6% compressive strength increase at 90 days, consistent with Semmana et al. [40] findings on glass powder densification effects. Group 2 (SCC–7.5% SS, Figure 9c) exhibited moderate microstructural improvements with well-dispersed reactive silica clusters and progressive C–S–H gel development, achieving 85.0% reduction in surface area (59.6 m²/g) and 75.9% reduction in pore volume (0.289 cc/g), corroborating the 23.8% strength increase at 90 days and supporting Jawad Ahmad et al. [47] findings on enhanced particle bonding and enhanced matrix packing through pozzolanic reactions. The hybrid systems indicated a complex microstructural interactions, with Group 3 (SCC–15% GP + 5% SS, Figure 9d) showing non-uniform glass particles distribution and inter-particle voids at standard water content (w/c = 0.39), resulting in 26.1% increase in surface area (292.67 m²/g) reflecting inefficient particle packing and clarifying reduced mechanical efficiency, while Group 4 (SCC–L–15% GP + 5% SS, Figure 9e) achieved optimal microstructural characteristics through water content reduction (w/c = 0.36) with interlocked C–S–H gel structures and ettringite crystals, resulting in 75.5% surface area reduction (96.91 m²/g) and enhanced early age strength development (55.5% increase at 7 days), supporting Mahmood et al. [46] and Raveendran et al. [38] findings that combining low water-to-binder ratios with hybrid pozzolanic additives leads to improvements in dense matrix formation and mechanical enhancement.

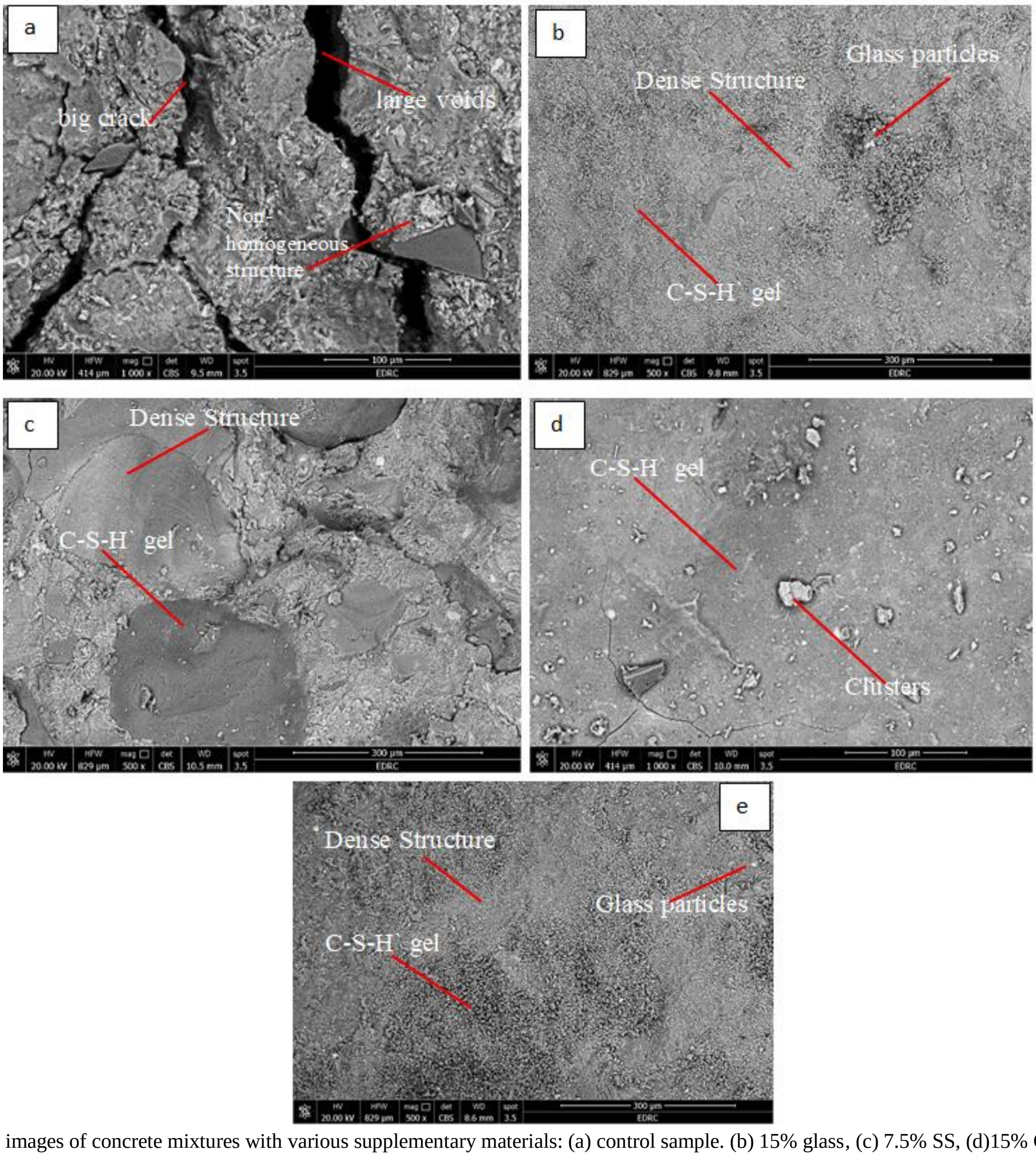

Figure 9: SEM images of concrete mixtures with various supplementary materials: (a) control sample. (b) 15% glass, (c) 7.5% SS, (d)15% GP +SS, and (e) 15% GP+ SS with a low water/cement ratio.

3.4.2 Stereo microscopic

Stereomicroscopic observation provided supporting findings on surface morphology, particle distribution, and interfacial bonding characteristics across all SCC mixtures. This technique offered enhanced depth perception and color differentiation, confirming the SEM findings while displaying additional textural features related to mechanical performance. The control sample (SCC–CON, Figure 10a) displayed rough surface texture characterized by non-uniform topography and extensive dark void spaces, directly connected to with low matrix integrity and illustrating the lowest compressive strength (28.5 MPa at 90 days). Group 1 (SCC–15% GP, Figure 10b) exhibited superior surface homogeneity with uniformly distributed glass particles observed as bright reflective spots, confirming excellent interfacial bonding and efficient particle packing, supporting the highest compressive strength (75 MPa at 90 days), consistent with Semmana et al. [40] findings on pore refinement and density enhancement due to from glass powder incorporation. Group 2 (SCC–7.5% SS, Figure 10c) showed improved surface characteristics with noticeable silica slurry clusters and localized reaction zones visible as areas of different coloration, indicating enhanced pozzolanic reactivity and resulting in compressive strength of 52 MPa at 90 days, consistent with Fode [48] documentation that reactive silica additions create zones with intensified packing within cement matrix. Group 3 (SCC–15% GP + 5% SS, Figure 10d) presented a finer textured surface distributed with visible small pores appearing as dark spots, indicating inadequate performance incorporation of hybrid additives, likely due to higher water content, corresponding with reduced compressive strength of 62 MPa at 90 days. Group 4 (SCC–L–15% GP + 5% SS, Figure 10e) achieved optimal surface morphology characterized by uniform texture distribution and distinctive discoloration patterns indicative of intense pozzolanic reactions between GP and SS, supporting exceptional early-age compressive strength of 65 MPa at 90 days. Overall, stereomicroscopic analysis confirmed that the most significant improvements in surface morphology and mechanical performance occurred in mixtures with optimized particle dispersion, adequate water-to-binder ratios, and enhanced pozzolanic activity, reinforcing the quantitative SEM findings regarding dense microstructural formation and pore structure refinement.

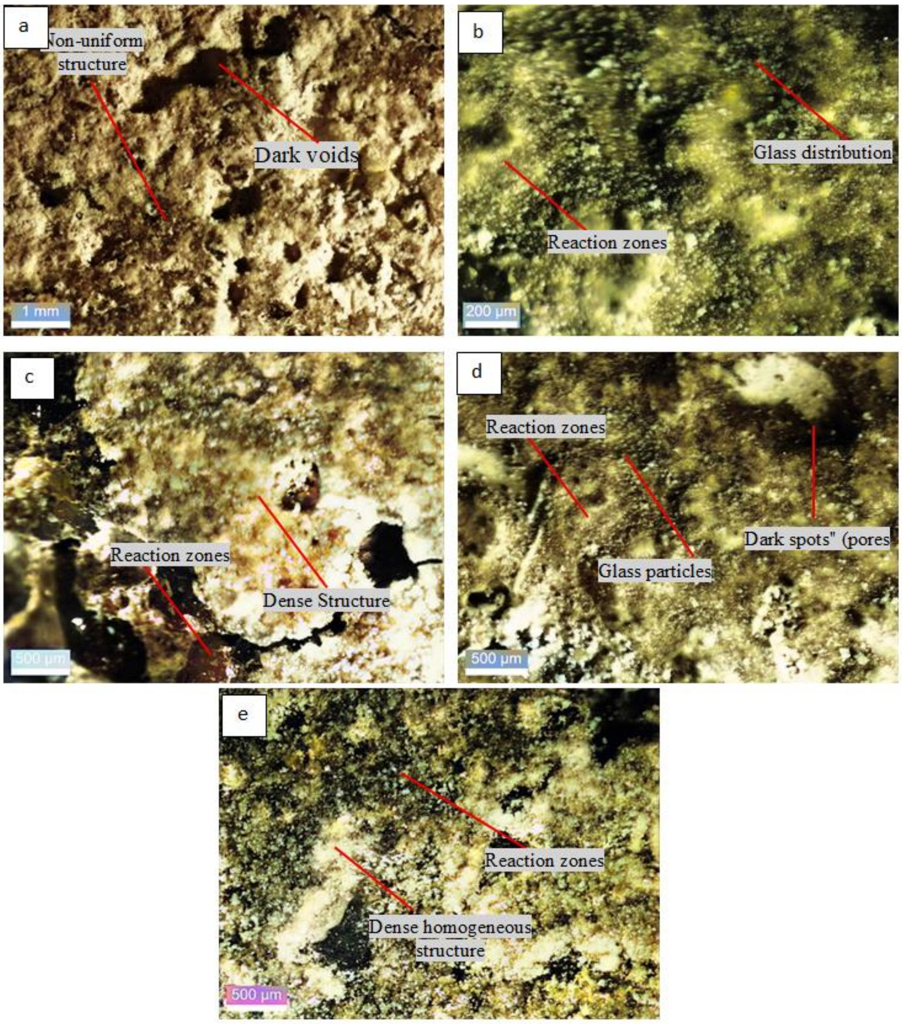

Figure 10: Stereo images of concrete mixtures with various supplementary materials: (a) control sample. (b) 15% glass, (c) 7.5% SS, (d)15% GP +SS, and (e) 15% GP+ SS with a low water/cement ratio.

3.4.3 X-ray diffraction (XRD)

Comprehensive XRD Peak Analysis and Phase Quantification for Supplementary Cementitious Materials in Self-Copamcting Concrete- ray diffraction (XRD) analysis examined the crystalline phase composition of five SCC mixtures to relate to hydration behavior and mechanical performance. Control Mix (SCC–CON, Figure 11a) established a control hydration profile with typical portlandite peaks at 2θ = 18.1° and 34.1°, and a calcite peak at 29.4°, where portlandite dominance indicates limited pozzolanic reaction and normal unmodified hydration route. Group 1 (SCC–15% GP, Figure 11b) exhibited increased C–S–H gel peaks at 2θ = 7.1°, 29.4°, and 50.1°, reduced portlandite peaks, and new crystalline C–S–H phase appearance at 23° and 38°, with phase composition of 69.10% orthoclase, 21.1% quartz, and only 2.4% portlandite. Specific decrease in portlandite accompanied by pozzolanic product formation (15–20%) confirmed intensive pozzolanic activity, as glass particles functioned as micro-fillers and reactive silica sources working effectively to transform portlandite to C–S–H by Islam et al. [4] and Shi et al. [7]. Group 2 (SCC–7.5% SS, Figure 11c) had ettringite formation peaks at 2θ = 9.0°, 15.8°, and 22.9° with reduced portlandite signals and phase composition of 76.5% orthoclase, 11% quartz, and 4.2% portlandite. Tobermorite-like C–S–H peak at 22.0° indicated increased pozzolanic reaction, while increased early strength due to ettringite formation reached a plateau after 56 days, most probably due to $Ca(OH)_2$ depletion and matrix densification, by Khan and Siddique [13]. Group 3 (SCC–15% GP + 5% SS, Figure 11d) had complex diffraction patterns with strong peaks at 2θ = 26.6° (quartz), 27.8° (orthoclase), and interference bands between 22° and 25°, with a phase composition of 84.9% orthoclase, 3.5% quartz, and 2.1% portlandite. Although high early strength, long-term strength was limited due to interfering reaction kinetics where glass powder slowly reacts but SS quickly reacts, causing early surface coating and preventing further hydration, consistent with Kumar et al. [49]. Group 4 (SCC–L–15% GP + 5% SS, Figure 11e) having optimum water content (w/c = 0.36) exhibited enhanced C–S–H peaks at 2θ = 7.1°, 29.4°, and 50.1°, and additional cementitious peaks at 31.8° and 45.5° and phase composition of 65.7% orthoclase, 9.1% quartz, and 2.4% portlandite, where enhanced crystalline structure indicates pozzolanic activity, particle distribution, and optimized hydration, consistent with Lothenbach et al. [50] identifying critical role of water-to-binder ratio and Pozzolanic synergy in strengthening durable cement matrices.

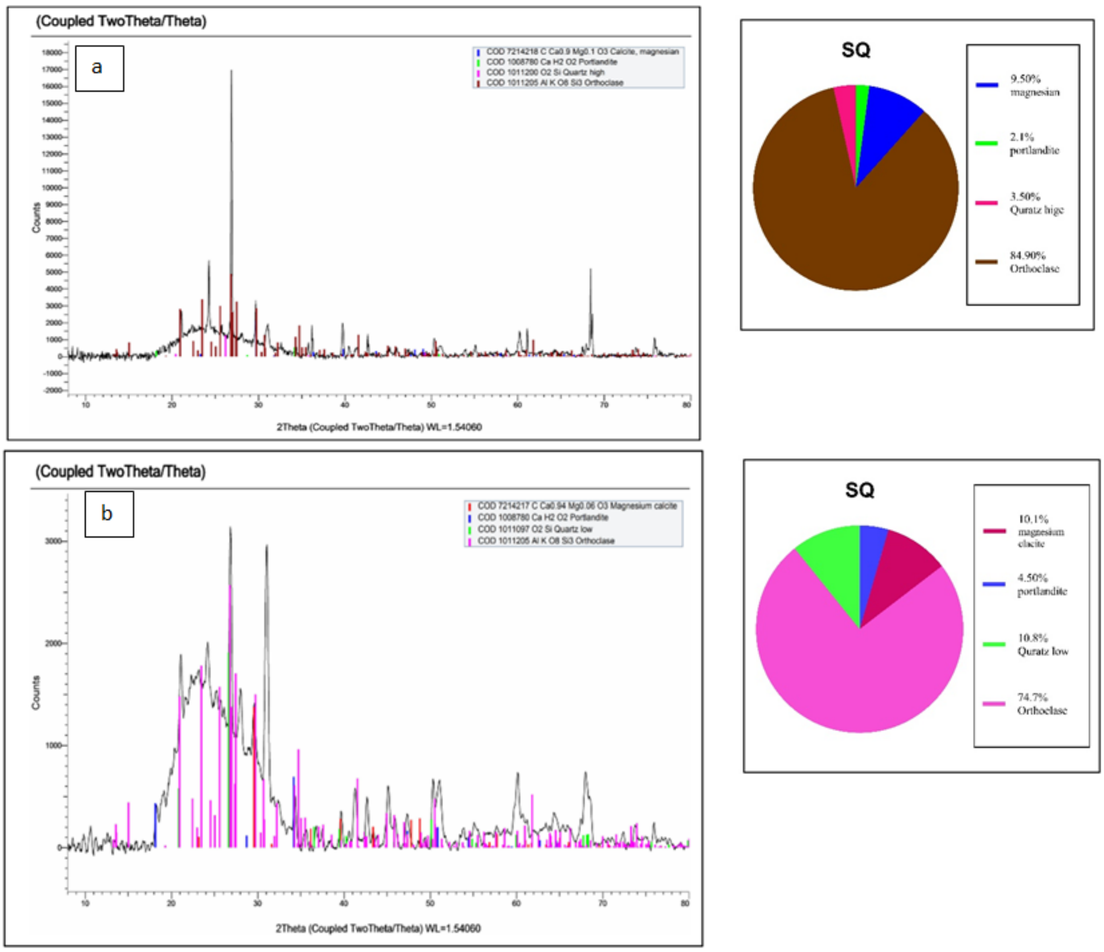

Figure 11: X-ray diffraction (XRD) patterns and phase composition of concrete mixtures with various supplementary cementitious materials: (a) Control mixture, (b) Glass powder (GP) mixture, (c) Silica slurry (SS) mixture, (d) Combined glass powder and silica slurry (GP+SS) mixture, and (e) Optimized GP+SS mixture.

3.4.4 X-ray Fluorescence (XRF)

X-ray fluorescence (XRF) analysis assessed the chemical content and oxide levels of SCC mixtures as presented in Table 5 by detecting characteristic X-ray emissions for the determination of significant oxides like SiO_2, CaO, Al_2O_3, and Fe_2O_3. The control mix (SCC-CON) contained 21% SiO_2 and 63% CaO, reflecting normal cement hydration with negligible pozzolanic reactivity and the lowest compressive strength. Group 1 (SCC-15% GP) had glass powder addition increased SiO_2 to 28.12% and decreased CaO to 56.10%, creating an optimized CaO/SiO_2 ratio that facilitated pozzolanic reactions in which amorphous silica reacts with calcium hydroxide to form additional C-S-H gel, and resulting strength gain of 24.1% at 7 days and 78.6% at 90 days, consistent with Omran and Tagnit-Hamou [51]. Group 2 (SCC-7.5% SS) had moderate changes in composition with SiO_2 increasing to 22.5% and CaO decreasing to 61%, recording strength increases of 11% at 7 days and 23.8% at 90 days, resulting from restricted pozzolanic action. Group 3 (SCC-15% GP + 5% SS) had peak SiO_2 levels of 28.5% and CaO levels of 56%, which conferred compressive strength gains of 40.7% at 7 days and 47.6% at 90 days due to synergistic pozzolanic reactions, as in Islam et al. [4]. Group 4 early strength high (SCC-L-15% GP + 5% SS) with low w/c ratio of 0.36 possessed ideal oxide composition and exhibited maximum strength gains of 55.6% at 7 days and 54.8% at 90 days by combined effects of optimal amount of SiO_2 and reduced water content, resulting in denser particle packing and reduced porosity. The results establish that water content minimization and chemical composition optimization significantly improve strength through heightened pozzolanic reactions and refinement in the microstructure, as established by Semmana [40] and Wang et al. [43].

3.4.5 Porosity Characteristics and Adsorption-Desorption Test

BET surface area and pore volume measurements (Figure 12) quantify pore structure, where higher values indicate greater porosity and reduced durability due to increased permeability. This technique evaluates how supplementary cementitious materials refine microstructure through void filling and denser matrix formation.

Control sample (SCC-CON, Figure 12a) revealed high BET surface area (396.2 m²/g) and pore volume (1.1977 cc/g) with well-connected capillary pores. This elevated value is typical for plain SCC without pozzolanic materials, where the lack of ultrafine particles and secondary C-S-H formation leads to larger interconnected pores.

Group 1 (SCC-15%GP, Figure 12b) achieved maximum refinement with 90.4% BET surface area reduction (38.2 m²/g) and 88.1% pore volume reduction (0.143 cc/g). Glass powder effectively suppressed pore connectivity through pozzolanic reactions, as identified by Bameri et al. [52]. **Group 2 (SCC-7.5%SS, Figure 12c)** demonstrated considerable improvement with 85.0% surface area reduction (59.6 m²/g) and 75.9% pore volume reduction (0.289 cc/g) through enhanced C-S-H development.

Group 3 (SCC-5%SS+15%GP, Figure 12d) surprisingly exhibited adverse effects, with a 26.1% increase in surface area (292.67 m²/g) and a 1.0% increase in pore volume (1.186 cc/g), indicating inefficient additive interaction that created larger pore networks. Sathiparan and Subramaniam [53] emphasized maintaining optimal hybrid ratios to avoid such effects. **Group 4 (SCC-L-5%SS+15%GP, w/c=0.36, Figure 12e)** exhibited 75.5% surface area reduction (96.91 m²/g) and 67.2% pore volume reduction (0.393 cc/g), demonstrating that reduced w/c ratio produces stronger, tighter pore networks. These results confirm that microstructural optimization depends on the effectiveness and compatibility of individual SCM. The superior performance of SCC-15%GP and optimized Group 4 confirms the significance of w/c ratio in achieving maximum SCM benefits, consistent with Lekhya and Kumar [54] findings on mix design optimization.

Table 5: Chemical composition of self-compacting concrete mixtures (%).

Oxide	No of Mixes				
	Scc-con	Scc-15% GP	Scc-7.5%ss	Scc-15% GP+5%SS	Scc-L-15% GP+5%SS (w.c%0.36%)
SiO_2	21.00%	28.12%	22.50%	28.50%	29.00%
	63.00%	56.10%	61.00%	56.00%	55.50%
Al_2O_3	5.00%	6.80%	5.80%	6.50%	6.80%
Fe_2O_3	3.00%	2.90%	3.20%	2.80%	2.90%
MgO	2.00%	1.90%	2.10%	1.90%	1.90%
SO_3	2.50%	2.30%	2.60%	2.20%	2.30%
Na_2O	0.30%	1.00%	0.40%	1.00%	1.00%
K_2O	0.70%	0.81%	0.70%	0.80%	0.80%
TiO_2	0.30%	0.30%	0.30%	0.30%	0.30%
P_2O_5	0.20%	0.20%	0.20%	0.20%	0.20%
Others	2.00%	1.80%	2.20%	1.80%	1.80%

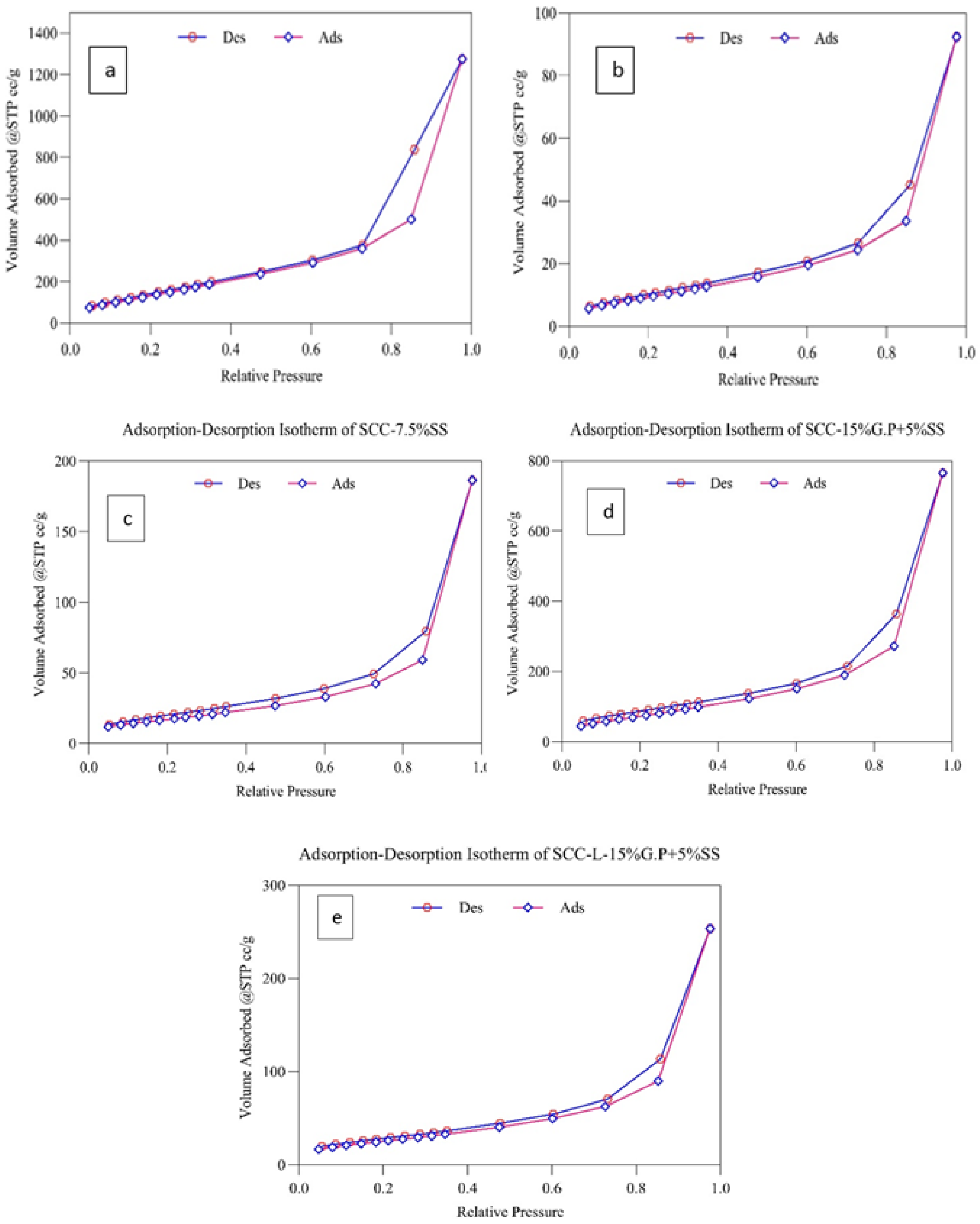

Figure 12: Adsorption-desorption isotherms of various Self-Compacting Concrete (SCC) Mixtures: (a) Control mixture, (b) Group 1 (15% glass powder), (c) Group 2 (7.5% silica slurry), (d) Group 3 (15% glass powder + 5% Silica slurry), and (e) Group 4 (15% glass powder + 5% Silica slurry).

3.4.6 Dynamic Light Scattering (DLS), size distribution, and polydispersity index (PDI)

Dynamic Light Scattering (DLS) analysis (Table 6, Figure 13) presents necessary data on particle size distribution and mixture homogeneity, improving the previously discussed microstructural characteristics and porosity findings. SCC–15% GP, related to Group 1, performed very well with an 89.8% reduction in particle size (5.6 µm) and a moderate PDI (0.04), again confirming the enhanced void-filling capability of glass powder. These observations are also supported by the notable reductions in BET surface area and total pore volume (Table 6, Figure 12b), in line with the improved compressive strength and overall durability.

SCC–7.5% SS in Group 2 showed the optimal particle uniformity (PDI = 0.03) with a particle size of 17 µm, which is beneficial for enhancing C–S–H gel development and improved surface morphology (Figure 12c). Ultrafine silica slurry enhanced particle dispersion and rate of hydration, as agreed with the microstructural benefits reported by Tavares et al. [55]. Group 3 (SCC–5%SS+ 15% GP) was more uniform (PDI=0.02) but worse in terms of particle size (35 µm), with greater than expected BET surface area (+26.1%) and pore volume (+1.0%) (Table 6, Figure 12d). This reduction is a result of excessive repulsive forces between particles and poor SCM interaction, supporting the concerns raised by Sathiparan and Subramaniam [53] regarding hybrid blend behavior. Group 4 (SCC–L–5% SS + 15% GP) showed balanced behavior associated with 15 µm particle size and modest PDI (0.05), along with significant decreases in BET surface area (–75.5%) and pore volume (–67.2%) (Table 6, Figure 12e). This finding confirms the requirement for water-to-cement ratio optimization to achieve improved particle packing and enhanced microstructural performance, as highlighted by Lekhya and Kumar [54]. Generally, Group 1 and Group 4 exhibited the most favorable characteristics, offering a combination of uniform particle distribution, minimal porosity, and superior packing efficiency. These features are essential for producing high-performance, durable SCC mixtures suitable for long-term structural applications.

Table 6: Polydispersity Index (PDI) and Dynamic Light Scattering (DLS) Measurements for Various Self-Compacting Concrete (SCC) Mixtures.

Sample (code)	PDI	PDI Classification	DLS
Scc-Cont.	0.08	High (Poor Uniformity)	55 µm
Scc-15% G. P	0.04	Medium	5.6 µm
Scc-7.5% SS	0.03	Low (Good Uniformity)	17 µm
Scc-5% SS+ 15% G. P	0.02	Very Low (Excellent Uniformity)	35 µm
Scc-L-5% SS+ 15% G.P	0.05	Medium	15 µm

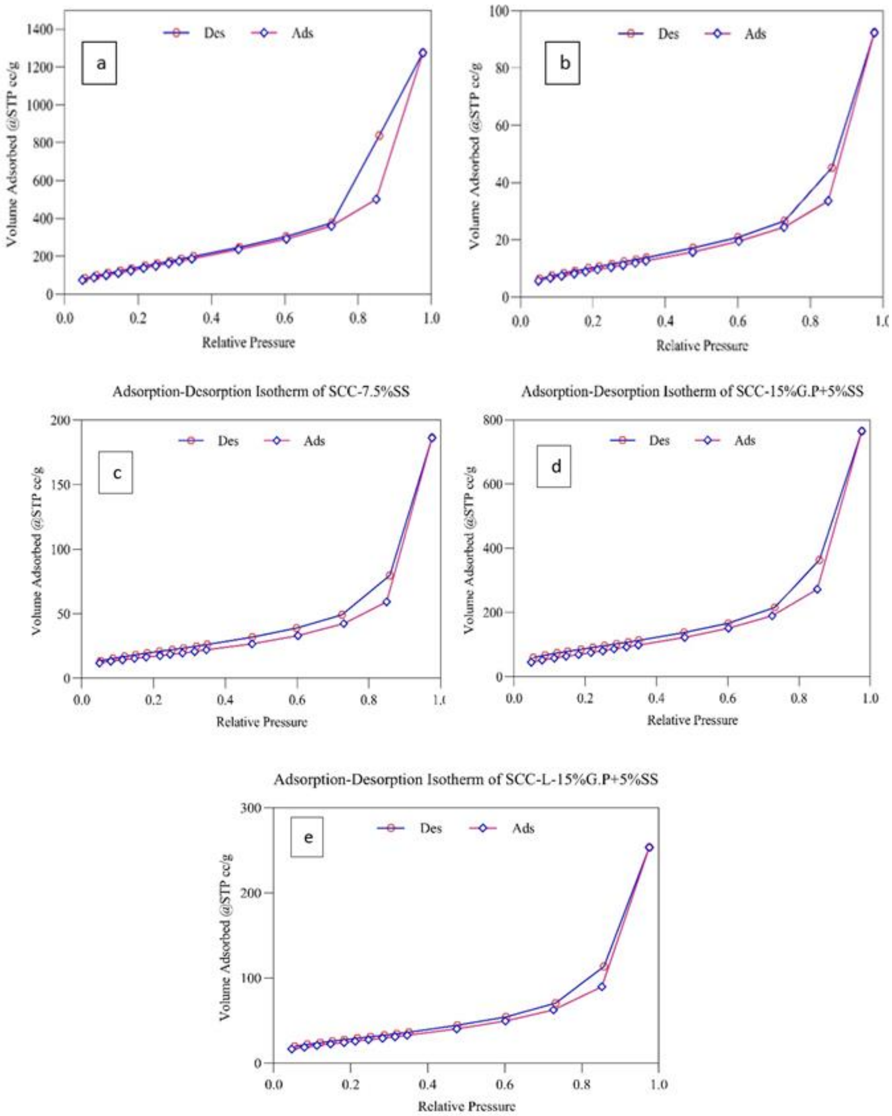

Figure 13: Dynamic Light Scattering (DLS) Test Results for Various Self-Compacting Concrete (SCC) Mixtures: : (a) Control mixture, (b) Glass powder (GP) mixture, (c) Silica slurry (SS) mixture, (d) Combined glass powder and silica slurry (GP+SS) mixture, and (e) Optimized GP+SS mixture.

4. Comparative Discussion and Research Contribution

A comprehensive review of the current findings in comparison with previous studies highlights the specific advancements provided by this work. Omran and Tagnit-Hamou [1] studied glass powder in self-compacting concrete and observed moderate strength enhancements (25% at 90 days), primarily due to physical filler effects and delayed pozzolanic reactivity. In contrast, the current study recorded a 78.6% increase in compressive strength at 90 days in SCC-15%GP, indicating more effective long-term hydration, attributed to optimized particle size distribution and improved water-to-cement ratio.

Regarding silica-based additives, said et al. [2] reported on the use of silica fume powder and noted difficulties with dispersion and water demand; these limitations were overcome here by using silica slurry in ultrafine suspended form, leading to notably improved fresh properties. Specifically, SCC-L-5%SS+15%GP achieved a slump flow of 710 mm compared to 555 mm in the control mix (SCC-CON), and reduced segregation due to synergistic interaction between the dispersive action of SS and the lubricating effect of the spherical GP particles. Mechanistically, the early strength gain of 55.6% at 7 days in SCC-7.5%SS is due to accelerated C–S–H formation driven by SS's high surface area and reactivity. Meanwhile, the gradual and sustained pozzolanic reaction of GP accounted for long-term pore refinement and strength development. This complementary behavior was most evident in the hybrid SCC-L-5%SS+15%GP mixture, which achieved balanced strength development (55.6% at 7 days, 54.8% at 90 days) and superior durability, with a 55% reduction in water absorption and 71% reduction in sorptivity. Compared to studies by Khatib [3] and Khan et al. [4], who analyzed the individual impacts of GP or SF, the present work presents an expanded framework through its integration of multi-scale microstructural tools (BET, XRD, DLS), which confirmed enhanced pore structure, reduced surface area, and improved CaO/SiO_2 ratios. Furthermore, while previous studies rarely applied this combination under controlled mix design conditions, this study closes a critical gap by showing how the hybrid use of SS and GP under optimized proportions produces SCC with superior mechanical, fresh, and durability performance suitable for high-demand applications.

5. Environmental Impact and Cost Analysis

Glass powder and silica slurry are two evolution-changing materials used in the production of sustainable concrete; these contribute to major environmental and economic benefits. The addition of ground glass powder reduces sand consumption by up to 15–20% and limits the use of natural aggregates, thereby minimizing the impacts of sand mining. Silica slurry, conversely, enables up to 15% replacement of cement, leading to enormously reduced CO_2 emissions during production. From an economic perspective, the raw material of ground glass powder is pricier ($1.45/kg) than silica slurry ($0.70/kg). However, when the costs of handling environmentally non-degradable glass waste are added, ground glass powder is a lower-cost option because of diversion and landfill savings.

Apart from cost reductions, glass powder enhances the compressive strength of concrete, whereas silica slurry enhances flowability and reduces the need for chemical admixture in self-compacting concrete. Overall, the result is the creation of durable, low-maintenance structures in line with the principles of the circular economy and lowering the environmental footprint of concrete production.

The selection between ground glass powder and silica slurry is finally based on local material availability, individual project requirements, and long-term performance preference. This may provide more benefits in regions with abundant waste glass and high landfilling costs, whereas silica slurry could be suitable in areas more practical for industrial applications**.**

6. Conclusions

This research has shown that the combined use of silica slurry (SS) and glass powder (GP) offers a major improvement in self-compacting concrete (SCC) performance, effectively overcoming the limitations of conventional cementitious systems. The application of silica slurry in the form of ultrafine suspended particles was markedly superior to dry silica powder, as it minimized particle agglomeration, lower water requirement, and ensured homogeneous dispersion throughout the matrix. Among the tested mixtures, SCC-L-5%SS+15%GP showed superior fresh properties, obtaining a slump flow of 710 mm, compared to 555 mm for the control mix (SCC-CON), and achieving a 38% improvement in segregation resistance due to the combined effects of SS dispersion and the lubricating spherical morphology of GP. In terms of mechanical performance, SCC-7.5%SS achieved notable early-age strength development, with a compressive strength gain of 55.6% at 7 days, due to accelerated C–S–H gel formation.

In contrast, SCC-15%GP provided the highest long-term strength, reaching a compressive strength increase of 78.6% at 90 days through sustained pozzolanic reactivity and progressive pore refinement.

The optimized hybrid mixture maintained balanced mechanical properties, with strength gains of 55.6% at 7 days and 54.8% at 90 days. Durability performance was markedly improved, as water absorption decreased by 55% and sorptivity was reduced by 71%, corroborated by BET, XRD, and XRF analyses confirming lower porosity, favorable CaO/SiO_2 ratios, and a refined microstructure. These outcomes provide clear evidence that combining silica slurry and glass powder in optimized proportions enables the production of self-compacting concrete with superior fresh workability, balanced strength development, and enhanced durability. This approach represents a scalable and cost-effective solution for sustainable concrete production, particularly in regions with high glass waste availability.

REFERENCES

[1] Jani, Y., & Hogland, W. (2014). Waste glass in the production of cement and concrete – A review. Journal of Environmental Chemical Engineering, 2(3), 1767-1775. .https://doi.org/10.1016/j.jece.2014.03.016

[2] Rashad, A. M. (2014). Recycled waste glass as fine aggregate replacement in cementitious materials based on Portland cement. Construction and Building Materials, 72, 340-357. https://doi.org/10.1016/j.conbuildmat.2014.08.092

[3] Lee, H., Hanif, A., Usman, M., Sim, J., & Oh, H. (2018). Performance evaluation of concrete incorporating glass powder and glass sludge wastes as supplementary cementing material. Journal of Cleaner Production, 170, 683–693. https://doi.org/10.1016/j.jclepro.2017.09.133

[4] Islam, G. M. S., Rahman, M. H., & Kazi, N. (2017). Waste glass powder as partial replacement of cement for sustainable concrete practice. International Journal of Sustainable Built Environment, 6(1), 37-44. https://doi.org/10.1016/j.ijsbe.2016.10.005

[5] Hamada, H., Alattar, A., Tayeh, B., Yahaya, F., & Thomas, B. (2022). Effect of recycled waste glass on the properties of high-performance concrete: A critical review. Case Studies in Construction Materials, 17, e01149. https://doi.org/10.1016/j.cscm.2022.e01149

[6] Shayan, A., & Xu, A. (2006). Performance of glass powder as a pozzolanic material in concrete: A field trial on concrete slabs. Cement and Concrete Research, 36(3), 457-468. https://doi.org/10.1016/j.cemconres.2005.12.012

[7] Shi, C., Wu, Y., Riefler, C., & Wang, H. (2005). Characteristics and pozzolanic reactivity of glass powders. Cement and Concrete Research, 35(5), 987-993. https://doi.org/10.1016/j.cemconres.2004.05.015

[8] Sobolev, K., Türker, P., Soboleva, S., & Iscioglu, G. (2007). Utilization of waste glass in ECO-cement: Strength properties and microstructural observations. Waste Management, 27(7), 971-976. https://doi.org/10.1016/j.wasman.2006.07.014

[9] Shao, Y., Lefort, T., Moras, S., & Rodriguez, D. (2000). Studies on concrete containing ground waste glass. Cement and Concrete Research, 30(1), 91-100. https://doi.org/10.1016/j.cemconres.2004.05.015

[10] Idir, R., Cyr, M., & Tagnit-Hamou, A. (2011). Pozzolanic properties of fine and coarse color-mixed glass cullet. Cement and Concrete Composites, 33(1), 19-29. https://doi.org/10.1016/j.cemconcomp.2010.09.013

[11] Matos, A. M., & Sousa-Coutinho, J. (2012). Durability of mortar using waste glass powder as cement replacement. Construction and Building Materials, 36, 205-215. https://doi.org/10.1016/j.conbuildmat.2012.04.027

[12] Siddique, R. (2011). Utilization of silica fume in concrete: Review of hardened properties. Resources, Conservation and Recycling, 55(11), 923-932. https://doi.org/10.1016/j.resconrec.2011.06.012

[13] Khan, M. I., & Siddique, R. (2011). Utilization of silica fume in concrete: Review of durability properties. Resources, Conservation and Recycling, 57, 30-35. https://doi.org/10.1016/j.resconrec.2011.09.016

[14] Mehta, P. K., & Monteiro, P. J. (2014). Concrete: Microstructure, Properties, and Materials (4th ed.). McGraw-Hill Education, New York, NY, USA. ISBN: 9780071797870

[15] Dunster, A. (2009). Silica Fume in Concrete. IHS BRE Press, Watford, UK. ISBN: 978-1848061057

[16] Sharifi, Y., Afshoon, I., Firoozjaei, Z., & Momeni, A. (2016). Utilization of waste glass micro-particles in producing self-consolidating concrete mixtures. International Journal of Concrete Structures and Materials, 10(3), 337-353. https://doi.org/10.1007/s40069-016-0141-z

[17] Esraa Emam Ali, Sherif H. Al-Tersawy,Recycled glass as a partial replacement for fine aggregate in self-compacting concrete, Construction and Building Materials, Volume 35,2012, Pages 785-791, ISSN 0950-0618. https://doi.org/10.1016/j.conbuildmat.2012.04.117

[18] Liu, M. (2011). Incorporating ground glass in self-compacting concrete. Construction and Building Materials, 25(2), 919-925. https://doi.org/10.1016/j.conbuildmat.2010.06.092

[19] Wang, H. Y., & Huang, W. L. (2010). Durability of self-consolidating concrete using waste LCD glass. Construction and Building Materials, 24(6), 1008-1013. https://doi.org/10.1016/j.conbuildmat.2009.11.018

[20] Zaichenko, N., Said, A. A., & Sakhoshko, E. (2011). Silica fume-based admixture in the form of aqueous slurry for self-compacting concrete. Materials Science and Engineering. Available at: https://api.semanticscholar.org/CorpusID:55229832

[21] Motahari Karein, S. M., Ramezanianpour, A. A., Ebadi, T., Isapour, S., & Karakouzian, M. (2017). A new approach for application of silica fume in concrete: Wet granulation. Construction and Building Materials, 157, 573-581. https://doi.org/10.1016/j.conbuildmat.2017.09.132

[22] Yasser Sharifi, Mahmoud Houshiar, Behnam Aghebati, (2013). Recycled glass replacement as fine aggregate in self-compacting concrete. Frontiers of Structural and Civil Engineering, 7(4), 419-428. https://doi.org/10.1007/s11709-013-0224-8

[23] Keerio, M.A., Abbasi, S.A., Kumar, A. (2022). Effect of Silica Fume as Cementitious Material and Waste Glass as Fine Aggregate Replacement Constituent on Selected Properties of Concrete. Silicon 14, 165–176. https://doi.org/10.1007/s12633-020-00806-6

[24] Abd El-Hameed, M. Z., Mohamed, O. M., Abo El-Kassem, M. H., & Al-Numani, M. T. (2022). Effect of using glass powder as a partial replacement of cement on concrete properties. Journal of Al-Azhar University Engineering Sector, 17(62), 219-236. https://doi.org/10.21608/auej.2022.216806

[25] Khatib, J. M., Negim, E. M., Sohl, H. S., & Chileshe, N. (2012). Glass powder utilization in concrete production. European Journal of Applied Sciences, 4(4), 173-176. https://idosi.org/ejas/4(4)12/6.pdf

[26] Nassar, R. U. D., & Soroushian, P. (2012). Strength and durability of recycled aggregate concrete containing milled glass as a partial replacement for cement. Construction and Building Materials, 29, 368-377. https://doi.org/10.1016/j.conbuildmat.2011.10.061

[27] Ramezanianpour, A. A., Dashti, P., Banar, R., Zolfagharnasab, A., & Ramezanianpour, A. M. (2020). Effect of using silica fume as blended cement and slurry on durability against sulfate attack and alkali-silica reaction. In International Conference on Concrete Sustainability. Available at: https://www.researchgate.net/publication/346572905

[28] Afshinnia, K., & Rangaraju, P. R. (2016). Impact of combined use of ground glass powder and crushed glass aggregate on selected properties of Portland cement concrete. Construction and Building Materials, 117, 263-272. https://doi.org/10.1016/j.conbuildmat.2016.04.072

[29] Tamanna, N., Tuladhar, R., & Sivakugan, N. (2020). Performance of recycled waste glass sand as partial replacement of sand in concrete. Construction and Building Materials, 239, 117804. https://doi.org/10.1016/j.conbuildmat.2019.117804

[30] Samir Saify, Mohammed Sattar Radhi, Samer A. Al-Mashhadi, Basim Mareai, Sarah Fadel Jabr, Zainab. (2023). Impact of waste materials (glass powder and silica fume) on features of high strength concrete, Open Engineering; 13: 20220479. https://doi.org/10.1515/eng-2022-0479

[31] Aliabdo, A.A., Abd Elmoaty, A.E.M., Aboshama, A.Y. (2016). Utilization of waste glass powder in the production of cement and concrete. Construction and Building Materials, 124, 866-877. https://doi.org/10.1016/j.conbuildmat.2016.08.016

[32] Arshad MT, Ahmad S, Khitab A, Hanif A. (2021). Synergistic Use of Fly Ash and Silica Fume to Produce High-Strength Self-Compacting Cementitious Composites. Crystals. 11(8):915. https://doi.org/10.3390/cryst11080915

[33] Said, A.M., Zeidan, M.S., Bassuoni, M.T., Tian, Y. (2012). Properties of concrete incorporating nano-silica. Construction and

Building Materials, 36, 838-844. https://doi.org/10.1016/j.conbuildmat.2012.06.044

[34] Du, H., Tan, K.H. (2015). Transport properties of concrete with glass powder as supplementary cementitious material. ACI Materials Journal, 112(3), 429-438. https://doi.org/10.14359/51687363

[35] Khan, K., Ahmad, W., Amin, M. N., Rafiq, M. I., Abu Arab, A. M. (2023). Alabdullah, I. A., Alabduljabbar, H., & Mohamed, A. "Evaluating the effectiveness of waste glass powder for the compressive strength improvement of cement mortar using experimental and machine learning methods." Heliyon, 9(5), e16288. DOI: https://doi.org/10.1016/j.heliyon.2023.e16288

[36] Yahia, Y., Alsharie, H., Suliman, M. and Masoud, T. (2017) Effects of Wood Ash and Waste Glass Powder on Properties of Concrete in Terms of Workability and Compressive Strength in Jaresh City. Open Journal of Civil Engineering, 7, 423-431. Doi: 10.4236/ojce.2017.73029.

[37] Badalyan, M. M., Muradyan, N. G., Shainova, R. S., Arzumanyan, A. A., Kalantaryan, M. A., Sukiasyan, R. R., Yeranosyan, M., Laroze, D., Vardanyan, Y. V., & Barseghyan, M. G. (2024). Effect of Silica Fume Concentration and Water–Cement Ratio on the Compressive Strength of Cement-Based Mortars. Buildings, 14(3), 757. https://doi.org/10.3390/buildings14030757

[38] Raveendran, Namitha & K, Vasugi. (2025). Engineering performance and environmental assessment of sustainable concrete incorporating nano silica and metakaolin as cementitious materials. Scientific Reports. 15. 10.1038/s41598-025-85358-8, DOI:10.1038/s41598-025-85358-8

[39] Paruthi, S., Rahman, I., Khan, A. H., et al. (2024). "Strength, durability, and economic analysis of GGBS-based geopolymer concrete with silica fume under harsh conditions." Scientific Reports, 14, 31572. DOI: https://doi.org/10.1038/s41598-024-77801-z

[40] Semmana, A., Benzaamia, M., Meddah, M. S., & Beddar, M. (2025). "A Systematic Review of the Strength, Durability, and Microstructure Properties of Concrete Incorporating Glass Powder." Engineering Reports, 7(1), e70002. DOI: https://doi.org/10.1002/eng2.70002

[41] Abraham, N. A., S, A., Das, A., K S, A., & P Sibi, D. (2024). "Rubber fiber reinforced geopolymer concrete with silica fumes as a replacement for fine aggregate." E3S Web of Conf., 529. DOI: https://doi.org/10.1051/e3sconf/202452901038

[42] Aruchamy, Vennila & Subramaniyan, Yuvaraj & Viswanathan, Rajeshkumar & Manoharan, Arunkumar. (2024). Improving durability and mechanical features of silica fume and waste glass powder in eco-friendly self-compacting concrete. Matéria (Rio de Janeiro). http://dx.doi.org/10.1590/1517-7076-rmat-2024-0072

[43] Wang, Jiangjiang & Yang, Yusen & Chu, Jiayin & Mo, Kim Hung & Yap, Pow Seng. (2023). Recent developments in utilization of nano silica in self-compacting concrete: A review. Structural Concrete. https://doi.org/10.1002/suco.202201054

[44] Kashyap, V.S., Sancheti, G., Yadav, J.S. (2023). Smart sustainable concrete: enhancing the strength and durability with nano silica. Smart Constr. Sustain. Cities 1, 20 (2023). https://doi.org/10.1007/s44268-023-00023-1

[45] Labaran, Y.H., Atmaca, N., Tan, M. (2024). Nano-enhanced concrete: unveiling the impact of nano-silica on strength, durability, and cost efficiency. Discov Civ Eng 1, 116 (2024). https://doi.org/10.1007/s44290-024-00120-9

[46] Mahmood, M.S., Ali, T., Inam, I. (2025). Machine learning prediction and explainability analysis of high strength glass powder concrete using SHAP PDP and ICE. Sci Rep 15, 22089 (2025). https://doi.org/10.1038/s41598-025-04762-2

[47] Jawad Ahmad, Mohanad Muayad Sabri, Ali Majdi, Wael Alattyih, Inamullah Khan, Muhammad Alam. (2024). Durability and microstructure aspects of sustainable concrete made with ceramic waste: a review. Frontiers in Materials, 11, 1508989. https://doi.org/10.3389/fmats.2024.1508989

[48] Fode, M. (2024). "Effect of Natural Pozzolana on Physical and Mechanical Properties of Concrete." Advances in Civil Engineering, 2024, 3356641. https://doi.org/10.1155/2024/3356641

[49] Kumar, S., García-Triñanes, P., Teixeira-Pinto, A., Bao, M. (2021). "Development of alkali activated cement from mechanically activated silico-manganese (SiMn) slag." Cement and Concrete Composites, 40, 7-13. https://www.sciencedirect.com/science/article/abs/pii/S0958946513000455

[50] Lothenbach, B., Scrivener, K., & Hooton, R. D. (2011). Supplementary cementitious materials. Cement and Concrete Research, 41(12), 1244-1256. https://doi.org/10.1016/j.cemconres.2010.12.001

[51] Omran, A., & Tagnit-Hamou, A. (2016). Performance of glass-powder concrete in field applications. Construction and Building Materials, 109, 84-95. https://doi.org/10.1016/j.conbuildmat.2016.02.006

[52] Bameri, S., Ghafari, E., & Sadrmomtazi, A. (2025). Influence of waste glass powder as a supplementary cementitious material (SCM) on the mechanical properties, expansion, environmental impact, and microstructure of cementitious mortar. Engineering Reports, 7(1), e70238. https://doi.org/10.1002/eng2.70238

[53] Sathiparan, N., & Subramaniam, D. N. (2025). Sustainable pervious concrete with silica fume as cement replacement: A review. Transportation Research Record, 2679(2), 156-167. https://doi.org/10.1177/03611981241265852

[54] Lekhya, A., & Kumar, N. (2024). A study on the effective utilization of ultrafine fly ash and silica fume content in high-performance concrete through an experimental approach. Heliyon, 10, e39678. https://doi.org/10.1016/j.heliyon.2024.e39678

[55] Tavares, L.R.C., Junior, J.F.T., Costa, L.M. (2020). Influence of quartz powder and silica fume on the performance of Portland cement. Sci Rep 10, 21461 (2020). https://doi.org/10.1038/s41598-020-78567-w